Crystal Structure of P450cin in a Complex with Its Substrate, 1,8-Cineole, a Close Structural Homologue to D-Camphor, the Substrate for P450cam[†,‡]

Yergalem T. Meharenna,[⊥,§] Huiying Li,[⊥,§] David B. Hawkes,[∥] Andrew G. Pearson,[∥] James De Voss,[∥] and Thomas L. Poulos*[,⊥,§,▽,#]

Department of Molecular Biology and Biochemistry, Department of Physiology & Biophysics, Department of Chemistry, and the Program in Macromolecular Structure, University of California, Irvine, Irvine, California 92697-3900, and Department of Chemistry, The University of Queensland, Brisbane, Queensland 4072, Australia

Received April 8, 2004; Revised Manuscript Received May 19, 2004

ABSTRACT: Cytochrome P450cin catalyzes the monooxygenation of 1,8-cineole, which is structurally very similar to D-camphor, the substrate for the most thoroughly investigated cytochrome P450, cytochrome P450cam. Both 1,8-cineole and D-camphor are C_{10} monoterpenes containing a single oxygen atom with very similar molecular volumes. The cytochrome P450cin−substrate complex crystal structure has been solved to 1.7 Å resolution and compared with that of cytochrome P450cam. Despite the similarity in substrates, the active site of cytochrome P450cin is substantially different from that of cytochrome P450cam in that the B′ helix, essential for substrate binding in many cytochrome P450s including cytochrome P450cam, is replaced by an ordered loop that results in substantial changes in active site topography. In addition, cytochrome P450cin does not have the conserved threonine, Thr252 in cytochrome P450cam, which is generally considered as an integral part of the proton shuttle machinery required for oxygen activation. Instead, the analogous residue in cytochrome P450cin is Asn242, which provides the only direct protein H-bonding interaction with the substrate. Cytochrome P450cin uses a flavodoxin-like redox partner to reduce the heme iron rather than the more traditional ferredoxin-like Fe_2S_2 redox partner used by cytochrome P450cam and many other bacterial P450s. It thus might be expected that the redox partner docking site of cytochrome P450cin would resemble that of cytochrome P450BM3, which also uses a flavodoxin-like redox partner. Nevertheless, the putative docking site topography more closely resembles cytochrome P450cam than cytochrome P450BM3.

Cytochromes P450 catalyze the monooxygenation of a vast array of molecules as follows:

$$R{-}H + NAD(P)H + O_2 + H^+ \rightarrow R{-}OH + NAD(P)^+ + H_2O$$

Electrons are transferred from NAD(P)H to the cytochrome P450 heme via a redoxin that contains either FMN[1] or Fe_2S_2 as a cofactor. Traditionally, cytochrome P450s have been grouped into two classes based on the types of redox partners utilized. Class I is represented by bacterial and mitochondrial P450s where electrons are shuttled from NADH to a FAD-containing ferredoxin reductase, which in turn reduces an Fe_2S_2 redoxin that binds and transfers electrons to the P450. Class II microsomal cytochrome P450s employ a single FAD/FMN protein called cytochrome P450 reductase that shuttles electrons from NADPH to the cytochrome P450 heme. Cytochrome P450BM3 is a bacterial variation on this theme where the cytochrome P450 and FAD/FMN reductase are fused together into a single polypeptide chain (*1*, *2*). Now, however, this simple classification appears to be too limited. Very recently a cytochrome P450 has been discovered that uses a fused FMN and Fe_4S_4 electron donor protein as a reductase that is linked to the C-terminal end of the cytochrome P450 (*3*). In addition, a new cytochrome P450, cytochrome P450cin, from *Citrobacter braakii* has been found that utilizes FAD- and FMN-containing proteins. Unlike microsomal cytochrome P450s, the FMN and FAD proteins are separate polypeptides (unpublished results). These last two P450s thus increase the number of P450 electron-transfer systems to four. In addition, those P450s that do not require a redox partner often are grouped together as a single class, which would increase the number of classes to five.

The substrate for cytochrome P450cin, 1,8-cineole (Figure 1), is produced by eucalyptus trees and is partly responsible

[†] This work was supported by NIH Grant GM33688 (T.L.P.).

[‡] The coordinates and the structure factors have been deposited in the Protein Data Bank (code 1T2B).

* To whom correspondence should be addressed. Phone: 1-949-824-7020. Fax: 1-949-824-3280. E-mail: poulos@uci.edu.

[⊥] Departments of Molecular Biology and Biochemistry, University of California, Irvine.

[§] Program in Macromolecular Structure, University of California, Irvine.

[∥] The University of Queensland.

[▽] Department of Physiology & Biophysics, University of California, Irvine.

[#] Department of Chemistry, University of California, Irvine.

[1] Abbreviations: cytochrome P450cin (CYP176A1), P450 from *Citrobacter braakii*; cytochrome P450cam (CYP101), P450 from *Pseudomonas putida*; cytochrome P450BM3 (CYP102), P450 from *Bacillus megaterium*; cytochrome P450eryF (CYP107A1), P450 from *Saccropolyspora erythraea*; FAD, flavin adenine dinucleotide; FMN, flavin mononucleotide.

10.1021/bi049293p CCC: $27.50
Published on Web 07/02/2004

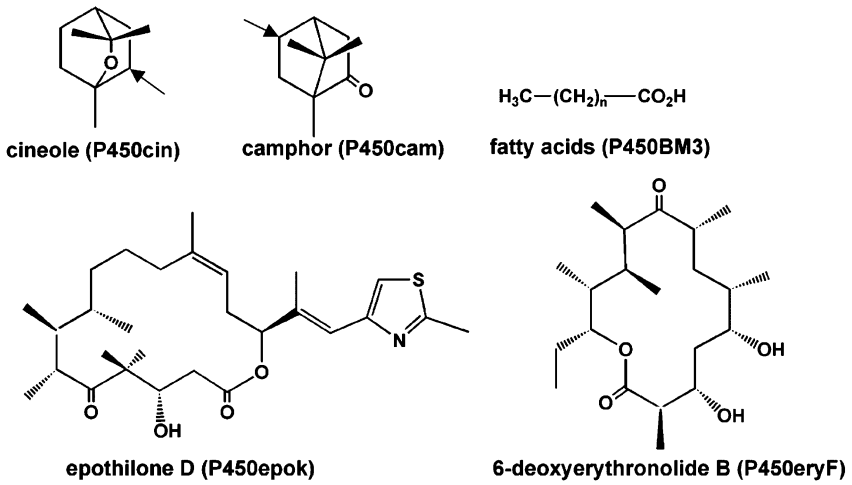

FIGURE 1: Chemical structures of substrates of bacterial cytochrome P450s. These substrates were used in solving the substrate complex structures of cytochrome P450cin (cineole), cytochrome P450cam (camphor), cytochrome P450BM3 (fatty acids), cytochrome P450epok (epothilone D), and cytochrome P450eryF (6-deoxyerythronolide B). The arrows indicate the carbons that are hydroxylated in cineole and camphor.

for the unique and pleasant odor associated with eucalyptus-derived essential oils. 1,8-Cineole is very similar in size and structure to D-camphor, the substrate for the most well-known and thoroughly investigated cytochrome P450, cytochrome P450cam. Thus far, the structures of cytochrome P450−substrate complexes that have been determined by X-ray crystallography are quite diverse with respect to the substrate structure (Figure 1). These structures have provided important insights into the range of variations required in the active site to achieve substrate selectivity. However, there are no structures of cytochrome P450s where the substrates are very similar. Thus, a comparison of the cytochrome P450cam and cytochrome P450cin structures provides an opportunity to unravel how two cytochrome P450s from quite different origins structurally adapt to the requirements of substrate specificity for substrates with very similar structure, size, and shape. A priori, it might be expected that the cytochrome P450cin and cytochrome P450cam active sites would be very similar. Despite the similarity in substrates, cytochrome P450cin is functionally quite different from cytochrome P450cam in that cytochrome P450cin uses a FMN-containing redox partner while cytochrome P450cam uses putidaredoxin or Pdx, an Fe_2S_2 ferredoxin-like protein. These similarities and differences with cytochrome P450cam make cytochrome P450cin an interesting target for structural studies and should broaden our understanding of the structural basis for substrate selectivity and redox partner recognition. Here we report the 1.7 Å structure of the cytochrome P450cin−substrate complex and compare this structure to that of cytochrome P450cam.

MATERIALS AND METHODS

Expression and Purification of Cytochrome P450cin. Cytochrome P450cin was expressed following a published protocol (*4*). The cell pellet was resuspended in 50 mM potassium phosphate, pH 7.4, 50 mM potassium chloride, 1 mM EDTA, 0.1 mM PMSF, 0.5 mM DTT, and 750 μM 1,8-cineole (buffer A). One microgram per milliter leupeptin and pepstatin A was added to buffer A. This was followed by cell lysis and incubation of the suspension with 1 mg/mL lysozyme for 1 h at 4 °C, followed by the addition of 8 mM $MgCl_2$ and 1 μg/mL DNase and further incubation for 1 h at 4 °C. The cell debris was removed by centrifugation for 1 h at 16 000 rpm at 4 °C. The cell-free supernatant then was loaded onto a DEAE Sepharose column equilibrated with buffer A. The bound protein was washed with three column volumes of buffer A and two column volumes of buffer A with 100 mM KCl, and the cytochrome P450 was eluted with buffer A in the presence of 300 mM KCl. The red-colored fractions were pooled and concentrated before loading onto a Sephacryl S200 gel filtration column equilibrated with buffer A. At this stage, the pooled fractions gave a single band of ~45 kD using SDS PAGE. The concentration of the substrate-bound protein was calculated by using $\epsilon = 132\ mM^{-1}\ cm^{-1}$ at 392 nm (*4*).

Crystallization. Crystallization of cytochrome P450cin was carried out using sitting drop vapor diffusion at room temperature. The sitting drops of 4 μL prepared by adding 2 μL of 40 mg/mL protein and 2 μL of well solution were equilibrated against a well solution comprised of 1.7 M sodium malonate, pH 6.0, overnight prior to macroseeding. A single plate crystal used for data collection was carefully separated from larger crystal clusters. Before crystals were frozen in liquid nitrogen for cryogenic data collection, crystals were transferred to a solution containing 2 M sodium malonate as cryoprotectant. Cytochrome P450cin crystals belong to the monoclinic space group $P2_1$, with unit cell parameters of $a = 62.4$ Å, $b = 68.96$ Å, $c = 105.550$ Å, and $\beta = 95.61°$.

Data Collection and Structure Determination. X-ray diffraction data were collected on beam line 5.0.2 at ALS (Berkeley, CA) using an ADSC Quantum 210 CCD detector. Optimization of data collection was guided by the STRATEGY function of MOSFLM (*5*). All data were reduced using DENZO and SCALEPACK, and rejections were performed with SCALEPACK (*6*).

The structure of cytochrome P450cin was solved using molecular replacement as implemented in MOLREP (*7*) using the polyalanine model of cytochrome P450cam (PDB accession number 1PHA) (*8*) as the search model. Two solutions were found with a correlation coefficient of 0.23 and $R = 0.64$ using data between 43 and 3.0 Å. Phases were

Table 1: Data Collection and Refinement Statistics

cell dimensions	a= 62.40 Å, b= 68.96 Å, c= 105.55 Å, β = 95.61°
space group	$P2_1$
data resolution (Å)	1.7
total observations	350 112
unique reflections	97 993
R_{sym}[a]	0.081 (0.451)[b]
$\langle I/\sigma \rangle$	6.8 (2.0)[b]
completeness	0.998 (1.00)[b]
redundancy	3.57
R factor[c]	0.225
R free[d]	0.262
no. of protein atoms	6292
no. of heteroatoms	104
no. of waters	990
RMS deviation	
bond length (Å)	0.01
bond angle (deg)	1.34
average B factor	21.3

[a] $R_{sym} = \sum|I - \langle I \rangle|/\sum I$, where I is the observed intensity and $\langle I \rangle$ $\iota\sigma$ the averaged intensity of multiple symmetry-related observations of the reflection. [b] The values in parentheses were obtained in the outermost resolution shell (1.72−1.69). [c] R factor $= \sum||F_o| - |F_c||/\sum|F_o|$; F_o and F_c are the observed and calculated structure factors, respectively. [d] R free was calculated with the 5% of reflections set aside randomly throughout the refinement.

improved and extended to 1.7 Å over 50 iterations of density modification using DM (*9*) including the solvent flattening procedure (*10*), as well as 2-fold noncrystallographic symmetry averaging. ARP/wARP calculations (*11*) through CCP4i user interface, using improvement of model by atoms update and refinement mode, were also carried out. The ARP/wARP-generated electron density map was of comparable quality to the map based on DM phases.

Beginning with the polyalanine cytochrome P450cam model, side chains of cytochrome P450cin were fit into the electron density map using the graphical model building program O (*12*). However, owing to displacement of some secondary structural elements in cytochrome P450cin compared to those in cytochrome P450cam, it was necessary to manually adjust stretches of backbone. This was followed by deletion of regions of the molecule that lacked clear backbone electron density. Once ~50% of the side chains were fit, a round of simulated annealing refinements with CNS (*13*) at 1.7 Å generated a much improved electron density map that enabled the construction of some difficult regions, including the N-terminus, the loop that replaced the B′ helix region, and the F/G-loop and G/H-loop regions.

The substrate, 1,8-cineole, was built and energy-minimized in Insight II and was included in the later stages of the CNS refinement. Waters were added using the WATERPICK routine during several additional rounds of refinement and model building. The final model contains a total of 7268 atoms, residues Met8−Glu404, heme, 1,8-cineole, and 990 water molecules. There are three *cis*-proline residues found in each molecule. The refined structure has R_{free} and R values of 26.2% and 22.5%, respectively. Backbone geometry was checked in PROCHECK (*14*). All of the residues fall into the allowed region in the Ramachandran plot with the only exception being Met90, which is well defined in clear density. The atomic coordinates have been deposited to the Protein Data Bank with the PDB code 1T2B. Data collection and refinement statistics are provided in Table 1. Volume

FIGURE 2: Ribbon diagram of cytochrome P450cin. The helices and β-sheets were assigned according to PROCHECK (*14*). The cytochrome P450cin X-ray structure shows a typical cytochrome P450 fold with a helix-rich domain on the right and a β-sheet-rich domain on the left. The unique ordered loop that replaces the B′ helix in cytochrome P450cam is indicated by an arrow.

calculations for the substrates and the substrate binding sites were performed using VOIDOO (*15*). The electrostatic surface potentials were calculated using GRASP (*16*). Figures were prepared with PYMOL (pymol.sourceforge.net), MOLSCRIPT (*17*), and RASTERED (*18*).

RESULTS AND DISCUSSION

Optical Spectra. The cytochrome P450cin used for crystallization exhibited the same spectral properties as reported by Hawkes et al. (*4*). The substrate-free protein gives the typical low-spin spectrum with a Soret peak at 415 nm. Upon binding of substrate, 1,8-cineole, the spectrum shifts to 100% high-spin with a peak at 392 nm owing to displacement of the axial water ligand by the substrate. The structure of 1,8-cineole and D-camphor are very similar because both are bicyclic C_{10} monoterpenes (Figure 1). However, D-camphor induced only a small (~20%) shift from low to high spin in cytochrome P450cin, and >100 μM D-camphor was required.

Overall Structural Comparison. Cytochrome P450cin has the traditional cytochrome P450 fold built around conserved four helical bundles in the core of the molecule (Figure 2). The closest structurally defined homologue to cytochrome P450cin is cytochrome P450cam (~26% sequence identity), and Figure 3 illustrates the difference in Cα positions between these two cytochrome P450s. Those regions with the lowest rms deviation are closest to the heme and include the cysteine-ligand region and helices I (residues 218−249) and L (residues 343−360). The largest differences (~5.5−6.2 Å) occur around residues 80−86, which form the B′ helix in cytochrome P450cam but are only a loop in cytochrome P450cin (Figure 4). The F−G loop (residues 169−172), the N-terminus (residues 8−42), and the N-terminal end of the G helix (residues 173−196) are also significantly different with a rms deviations ranging from 2.4 to 5.7 Å. Large differences in the B′ helix region and the F and G helices are normally observed in cytochrome P450s because these

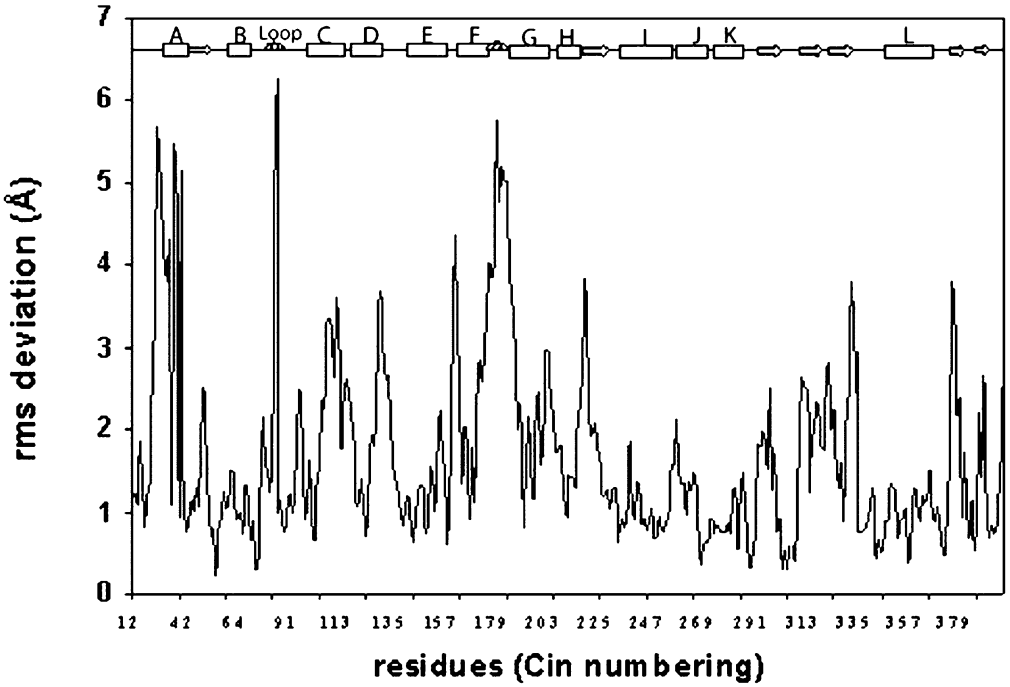

FIGURE 3: The rms deviation of Cα backbones between cytochrome P450cam and cytochrome P450cin plotted against the residue numbers of cytochrome P450cin. The backbone coordinates of cytochrome P450cam and P440cin were superimposed using the program LSQMAN. There is a major difference around the B′ helix of cytochrome P450cam, which is replaced by a well ordered loop in cytochrome P450cin.

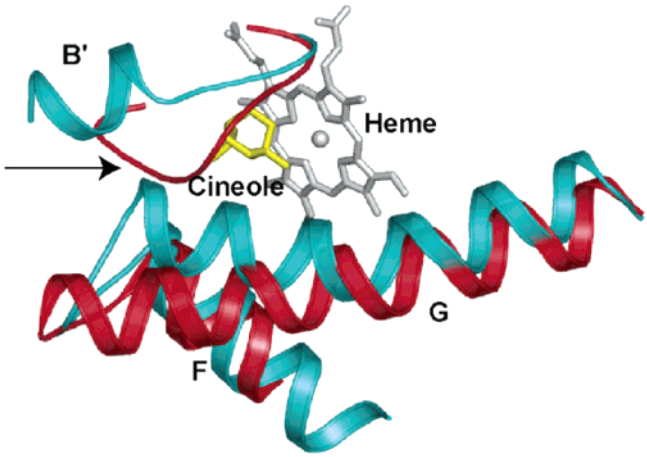

FIGURE 4: Superimposition of P450cin (red) and P450cam (cyan) showing the F and G helices and the P450cam B′ helical region all of which define the substrate access channel. The arrow highlights the region where P450cam has the B′ helix while P450cin has an ordered loop.

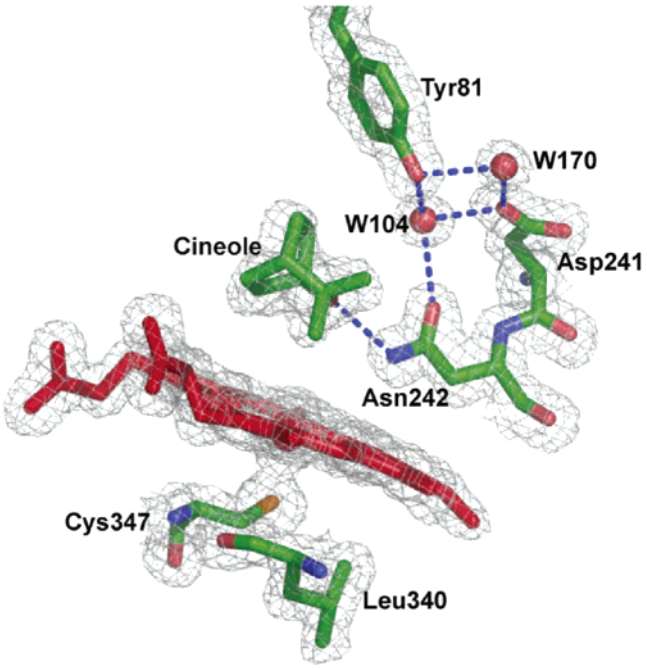

FIGURE 5: $2F_o - F_c$ composite omit map contoured at 1.0σ of the substrate and its immediate surroundings. Hydrogen bonds are indicated by dashed lines. Asn242, which replaces Thr252 in cytochrome P450cam, donates a hydrogen bond to the substrate (1,8-cineole) ether oxygen. An ordered water molecule (W104) makes hydrogen bonds bridging between Tyr81, which is located in the loop region that corresponds to the B′ helix of cytochrome P450cam, and Asn242. The conserved acidic residue on the I helix in cytochrome P450s, Asp242 in cytochrome P450cin, also makes a hydrogen bond with a water molecule (W170). The residue located adjacent to the Cys347 (cysteine ligand) and shielding the heme proximal face is a phenylalanine conserved in most other cytochrome P450s but substituted by Leu340 in cytochrome P450cin.

regions provide an entry channel for substrates as well as providing key substrate contact points.

Heme Environment. As in all cytochrome P450s, the proximal heme cysteine ligand, Cys347 in cytochrome P450cin, is situated near the N-terminal end of the proximal L helix (Figure 5), and the sulfur of the cysteine ligand accepts one H-bond from a peptide NH group, Gly349 in cytochrome P450cin. The one unique structural feature in cytochrome P450cin is Leu340 (Figure 5), which is situated adjacent to Cys347 and contacts the proximal surface of the heme. In all other known cytochrome P450 structures, this residue is phenylalanine. Studies on P450BM3 mutants (Phe393Ala, Phe393His), showed that the phenylalanine is not essential for electron transfer to the heme or for stabilizing heme binding (*19*). However, the conserved phenylalanine residue was observed to play an important role in the control of the reduction potential.

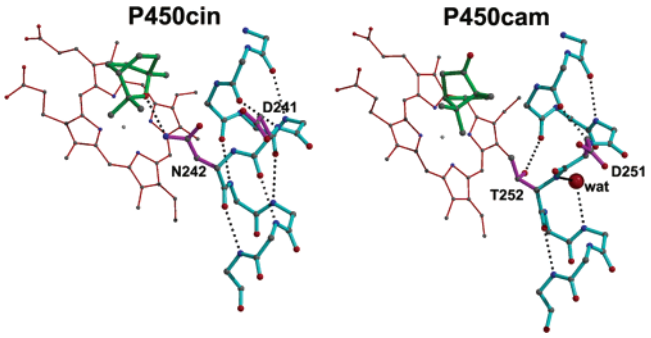

FIGURE 6: Comparison of the I helix in cytochrome P450cin and cytochrome P450cam. Hydrogen bonds are indicated by dashed lines. Note that the I helix kink is more pronounced in cytochrome P450cam, which leaves a large enough opening in the helix to accommodate a water molecule.

I Helix. In the majority of known cytochrome P450 structures, the I helix is the longest helix in the structure and runs over the distal surface of the heme. A local break in the normal α-helical hydrogen-bonding pattern forces the I helix to kink near the site of O_2 binding. In cytochrome P450cam, two key residues, Asp251 and Thr252, are situated at this local helical distortion, and both residues are thought to be essential for the proper delivery of solvent protons to the iron-linked O_2 molecule *(8, 20*−*23)*. Thr252 in cytochrome P450cam also plays an important structural role, since the Thr252 side chain OH donates a H-bond to the carbonyl oxygen of Gly248 (Figure 6). In a normal helix, Gly248 would H-bond with the peptide NH of Thr252, but the distance between these potential H-bonding partners is 4.7 Å owing to the local widening of the helical groove. This kink in the I helix provides an opening into which an ordered water molecule is situated to satisfy some of the missing helical H-bonds (Figure 6). The I helix kink is not nearly as pronounced in cytochrome P450cin (Figure 6). One reason is that Asn242 in cytochrome P450cin replaces the conserved Thr252 in cytochrome P450cam. Asn242 does not serve a similar structural role since the bulkier Asn242 side chain is oriented away from the I helix and toward the substrate where the Asn242 side chain provides the only H-bonding interaction with the substrate (Figures 5 and 6). Moreover, the Asn242 peptide NH accepts a normal H-bond from the peptide carbonyl oxygen of Gly238. As a result, the I helix in cytochrome P450cin does not widen as much as that in cytochrome P450cam leaving insufficient room for a solvent molecule.

Such subtle differences are important since Thr252 and the local solvent are key elements in providing the proper proton shuttle machinery required for reduction and activation of the iron-linked dioxygen (*24*). Cytochrome P450cin provides a variation on this theme given that Thr252 is replaced by Asn242 and the local solvent structure is quite different. Cytochrome P450eryF is another example of a cytochrome P450 with a non-cytochrome P450cam proton shuttle mechanism. Here Thr252 is replaced by alanine and the substrate itself provides the missing threonine OH group (*25*). Precisely how cytochrome P450cin compensates for the missing threonine OH group is unclear. Perhaps Asn242 serves a dual function in both anchoring the substrate in place and assisting in proton delivery. Alternatively, the ether oxygen of the substrate may play a part in directing proton delivery. The other key I helix residue generally considered

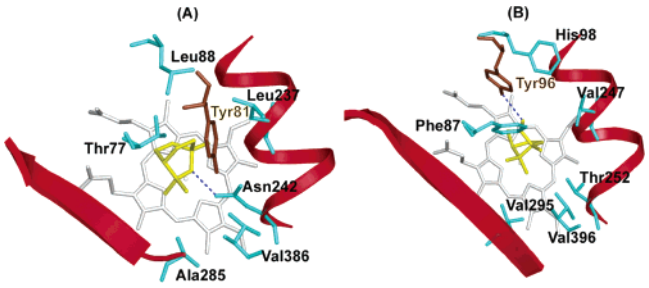

FIGURE 7: A comparison between the cytochrome P450cin (A) and cytochrome P450cam (B) active sites. Residues in cyan are those with a one-to-one correspondence in position but not identity between the two structures. The two tyrosine residues that are unique to each cytochrome P450 are brown.

to be important in oxygen activation, Asp251 in cytochrome P450cam (*23, 26*), is conserved in cytochrome P450cin (Asp241). Asp241 ion pairs with Arg239, as well as a cluster of solvent molecules. This is similar to cytochrome P450cam where Asp251 makes salt bridges with Arg186 in the F/G loop and Lys178 in the F helix, although Asp251 in cytochrome P450cam is less solvent-exposed.

Substrate Binding Region. The B′ helix region provides key substrate contact points in cytochrome P450s. We were somewhat surprised to find that the B′ helix is absent in cytochrome P450cin and instead is replaced by a loop that is well defined in the electron density map. Since this loop in cytochrome P450cin contacts the F and G helical regions, the G helix and F/G loop are pushed out further from the active site compared to those in cytochrome P450cam (Figure 4). Such large differences were unexpected owing to the striking similarity in the two substrates, D-camphor and 1,8-cineole (Figure 1). Both bicyclic monoterpenes have essentially the same molecular volumes, 33.59 and 33.33 $Å^3$, respectively. The internal volume of the substrate pocket calculated with VOIDOO also is very much the same, 256 and 264 $Å^3$ for cytochrome P450cin and cytochrome P450cam, respectively.

1,8-Cineole is anchored in place primarily by nonpolar interactions with the exception of the substrate ether oxygen atom, which accepts a H-bond from Asn242 (Figures6 and 7). 1,8-Cineole is positioned such that the atom to be hydroxylated (Figure 1) is about 5 Å from the iron compared to 4.2 Å in P450cam. In those substrate−protein contact regions where the secondary structural elements are conserved between P450cin and P450cam, there is in general a one-to-one correspondence in the location, but not identity, of residues contacting the substrate (Figure 7). For example, those residues forming the nonpolar substrate pocket in P450cin, Thr77, Leu88, Leu237, Val386, and Ala285, correspond to Phe87, Phe98, Val247, Val396, and Val295, respectively, in P450cam. The main difference is in the location of one key tyrosine residue in each cytochrome P450. Tyr96 in the cytochrome P450cam is part of the B′ helix and provides the only H-bond to the camphor carbonyl oxygen atom. Tyr81 in cytochrome P450cin indirectly aids in substrate binding by H-bonding to Asn241 via a bridging water molecule (Figure 5). Tyr81 is part of the loop that replaces the B′ helix in cytochrome P450cam, and there is no structural homologue in cytochrome P450cam. Owing to the similar size and shape of substrates, we had anticipated that only a handful of mutations would be required to

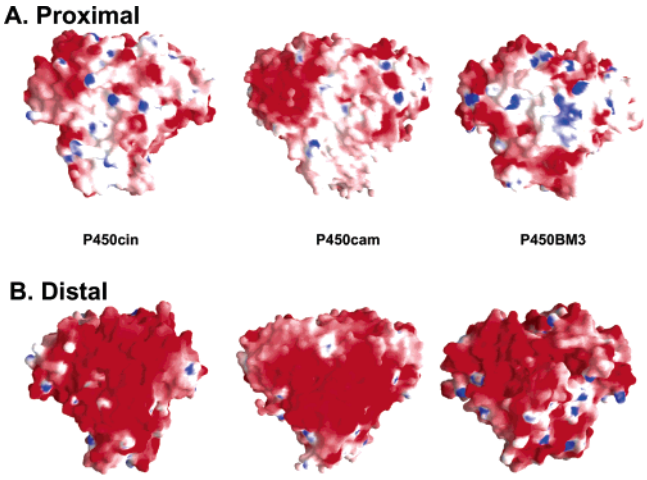

FIGURE 8: Electrostatic surface potential of the cytochrome P450cin, cytochrome P450cam, and cytochrome P450BM3 at ±8 kcal/mol, where the positive potential is shown in blue, negative potential in red, and neutral in white. The top view in panel A is on the proximal surface, the putative docking site for redox partners where heme has the closest approach to the protein surface. The panel B is viewed on the distal surface. This figure was prepared with GRASP (*16*).

interchange the substrate selectivity of cytochrome P450cam and cytochrome P450cin.

Interaction with the Redox Partner. One of the more interesting and unusual features of cytochrome P450cin is that this is the first, and to date only, bacterial cytochrome P450 that utilizes a FMN-containing flavodoxin-like redoxin (cindoxin) as its immediate electron donor. In contrast, cytochrome P450cam utilizes an Fe_2S_2 ferrredoxin-like protein, putidaredoxin, Pdx (*27*). The other bacterial cytochrome P450 known to utilize a FMN-containing donor is cytochrome P450BM3, although in this case the cytochrome P450 heme and reductase domains are linked together as a single polypeptide chain. Additionally the reductase domain of P450BM3 is analogous to cytochrome P450 reductase, the redox partner utilized by microsomal P450s. The one known structure of a cytochrome P450 electron-transfer complex is that of the cytochrome P450BM3 heme domain complexed to its FMN domain (*28*). The FMN domain docks on the proximal surface of the protein where it has closest approach from the molecular surface to the heme via a cysteine thiolate ligand containing loop. This also is the same region at which putidaredoxin is thought to bind to cytochrome P450cam (*29*−*31*). Electrostatic interactions are generally considered to be important in the binding of redox partners. The electrostatic surface potential of cytochrome P450cin, cytochrome P450cam, and cytochrome P450BM3 are shown in Figure 8. All three cytochrome P450s have a similar electropositive patch over the heme surface that very likely is used to interact with the electronegative redox partner (Figure 8A). Another factor contributing to redox partner recognition is the asymmetry of charge, which can generate substantial dipole moments, which also are important for recognition and binding. All three P450s under discussion here have a large electronegative patch on the distal surface (Figure 8B), which generates a dipole oriented toward the L helix on the proximal surface where redox partners bind. The computed dipole moment for cytochrome P450cin, 869 D, is larger than that for cytochrome P450cam, 679 D, and cytochrome P450BM3, 640 D.

We next examined in more detail the structure forming the redox partner docking site. Given the similarity in redox partners, it might be anticipated that the proximal surface docking site in cytochrome P450cin would more closely resemble that of cytochrome P450BM3 and the structurally related microsomal cytochrome P450s than that of cytochrome P450cam. However, a comparison of the docking surfaces (Figure 9) shows just the opposite: cytochrome P450cin more closely resembles cytochrome P450cam than cytochrome P450BM3. This is due primarily to the longer J helix and an extra J′ helix, as well as an insertion in the meander region in cytochrome P450BM3 relative to cytochrome P450cin and cytochrome P450cam that generates a more pronounced concave docking site in cytochrome P450BM3. However, all three proteins have a conserved residue important for redox partner binding located at the same position. Arg112 in cytochrome P450cam has been shown to be important for electron transfer and is thought to directly interact with its redox partner (*29*−*31*). Cytochrome P450cin also has an arginine (Arg102) at the location. The corresponding residue in cytochrome P450BM3 is His100 (Figure 9), and the structure of the cytochrome P450BM3 redox complex shows that His100 provides one of the few direct side chain intermolecular contacts with the FMN domain (*28*). Hence, we anticipate that Arg102 in cytochrome P450cin may well play a similar role in forming a redox complex with cindoxin.

CONCLUSIONS

To date, cytochrome P450cin is the closest homologue to cytochrome P450cam with respect to the size, shape, and chemical composition of the substrates, camphor vs 1,8-cineole, whose X-ray structure is known. Nevertheless, secondary structural elements forming key substrate contact points are substantially different. The key difference is the location of the protein hydrogen-bonding partner. Tyr96 in cytochrome P450cam, which hydrogen bonds with camphor, is next to the B′ helix, whereas the key residue that forms a hydrogen bond with 1,8-cineole is Asn242 from the I helix in P450cin. Cytochrome P450cin also has a tyrosine in the active site, Tyr81, although in this case Tyr81 does not directly contact the substrate. Instead, Tyr81 hydrogen bonds with Asn242 via a bridging water molecule. Despite these differences, it is somewhat surprising that D-camphor induces only a slight low to high spin shift. The absence of the Tyr96 hydrogen bond to camphor cannot be the main reason that camphor does not bind to cytochrome P450cin, since the Tyr96Phe in cytochrome P450cam mutant still binds camphor albeit with a 2-fold increase in K_d (*32*). Presumably, the difference in affinity between D-camphor and cineole is due to the location of the tyrosine protein hydrogen bonding partner and the sum of more subtle binding effects generated by the precise tailoring of the shape of the active site of cytochrome P450cin. Like cytochrome P450cam, cytochrome P450cin is expected to utilize a rigid network of active site H-bonds to deliver solvent protons to the heme-oxy complex for oxygen activation. Nevertheless, the structural details of how this is achieved in cytochrome P450cin must be quite different. Cytochrome P450cin lacks Thr252 (cytochrome P450cam numbering), which is generally considered important for the proton shuttle machinery, and instead has Asn242, which provides the only hydrogen bond to the substrate.

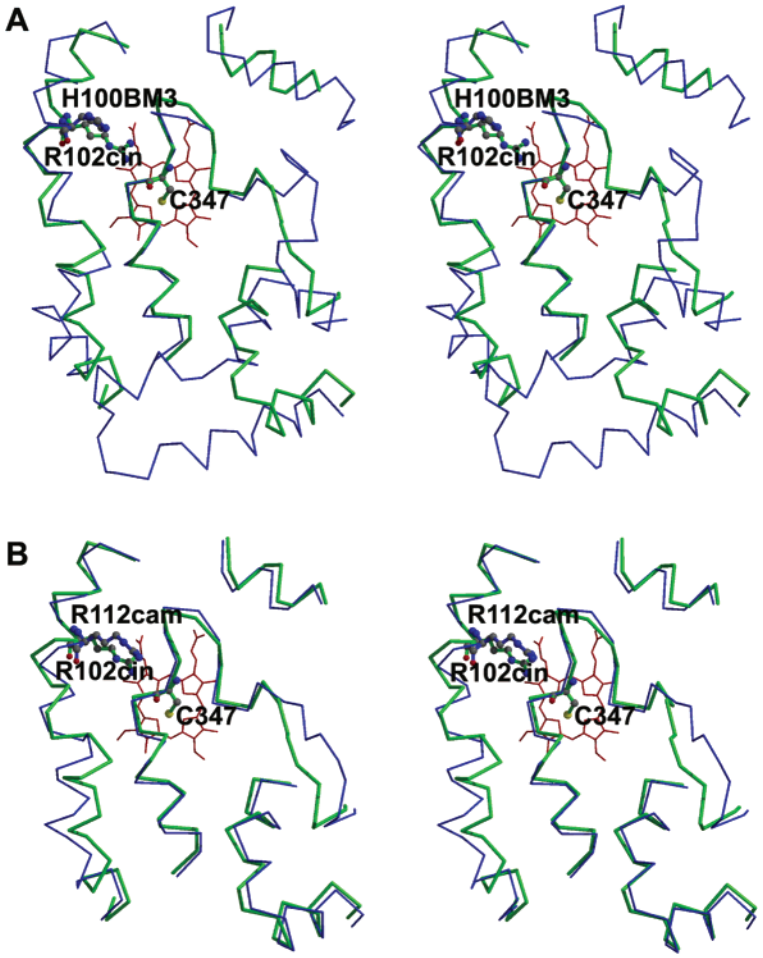

FIGURE 9: Stereodiagram showing a comparison between cytochrome P450cin (green) and cytochrome P450BM3 (panel A in blue) or cytochrome P450cam (panel B in blue). Key residues known to be important for redox partner binding are indicated.

Structures of diatomic complexes, especially the oxy-complex, will be required to shed more light on this point. Finally, the redox partner docking site in cytochrome P450cin more closely resembles cytochrome P450cam than cytochrome P450BM3 even though cytochrome P450cin uses a FMN-containing redox partner rather than an Fe_2S_2-containing partner. This provides an important variation that can, hopefully, enable a deeper understanding of redox partner recognition and electron transfer.

REFERENCES

1. Narhi, L. O., and Fulco, A. J. (1987) Identification and characterization of two functional domains in cytochrome P-450BM-3, a catalytically self-sufficient monooxygenase induced by barbiturates in *Bacillus megaterium*, *J. Biol. Chem. 262*, 6683−6690.
2. Narhi, L. O., Wen, L. P., and Fulco, A. J. (1988) Characterization of the protein expressed in *Escherichia coli* by a recombinant plasmid containing the *Bacillus megaterium* cytochrome P-450BM-3 gene, *Mol. Cell. Biochem. 79*, 63−71.
3. Roberts, G. A., Celik, A., Hunter, D. J. B., Ost, T. W. B., White, J. H., Chapman, S. K., Turner, N. J., and Flitsch, S. L. (2003) A self-sufficient Cytochrome P450 with a Primary Structural Organization That Includes a Flavin Domain and (2Fe-2S) Redox Center, *J. Biol. Chem. 278*, 48914−48920.
4. Hawkes, D. B., Adams, G. W., Burlingame, A. L., Ortiz de Montellano, P. R., and De Voss, J. J. (2002) Cytochrome P450cin (CYP176A), Isolation, expression, and characterization, *J. Biol. Chem. 277*, 27725−27732.
5. Leslie, A. G. W. (1992) MOSFLM, *Jt. CCP4 ESF-EACMB News Lett. Protein Crystallogr. 26*.
6. Otwinowski, Z., and Minor, W. (1997) Processing of X-ray diffraction data collected in oscillation mode, *Methods Enzymol. 276*, 307−326.
7. Vagin, A., and Teplyakov, A. (1997) MOLREP: an automated program for molecular replacement, *J. Appl. Crystallogr. 30*, 1022−1025.
8. Poulos, T. L., Finzel, B. C., and Howard, A. J. (1987) High-resolution crystal structure of cytochrome P450cam, *J. Mol. Biol. 195*, 687−700.
9. Cowtan, K. (1994) dm: an automated procedure for phase improvement by density modification, *Jt. CCP4 ESF-EACBM News Lett. Protein Improvement by Density Modification 31*, 34−38.
10. Wang, B. C. (1985) Resolution of phase ambiguity in macromolecular crystallography, *Methods Enzymol. 115*, 90−112.
11. Perrakis, A., Harkiolaki, M., Wilson, K. S., and Lamzin, V. S. (2001) ARP/wARP and molecular replacement, *Acta Crystallogr. D57*, 1445−1450.
12. Jones, T. A., Zou, J. Y., Cowan, S. W., and Kjeldgaard, M. (1991) Improved methods for building protein models in electron density maps and the location of errors in these models, *Acta Crystallogr. A47*, 110−119.
13. Brunger, A. T., Adams, P. D., Clore, G. M., DeLano, W. L., Gros, P., Grosse-Kunstleve, R. W., Jiang, J.-S., Kuszewski, J., Nilges, M., Pannu, N. S., Read, R. J., Rice, L. M., Simonson, T., and Warren, G. L. (1998) Crystallography & NMR System: A new software suite for macromolecular structure determination, *Acta Crystallogr. D54*, 905−921.
14. Laskowski, R. A., MacArthur, M. W., Moss, D. S., and Thornton, J. M. (1993) PROCHECK − A program to check stereochemcial quality of protein structures, *J. Appl. Crystallogr. 26*, 283−291.
15. Kleywegt, G. J., and Jones, T. A. (1994) Detection, Delineation, Measurement and Display of Cavities in Macromolecular Structures, *Acta Crystallogr. D50*, 178−185.

16. Nicholls, A., Sharp, K., and Honig, B. (1991) Protein folding and association: Insight from the interfacial and thermodynamic properties of hydrocarbons, *Proteins 11*, 281−296.
17. Kraulis, P. J. (1991) Molscript − a Program to Produce Both Detailed and Schematic Plots of Protein Structures, *J. Appl. Crystallogr. 24*, 946−950.
18. Merritt, E. A., and Murphy, M. E. P. (1994) Raster3d Version-2.0 − a Program for Photorealistic Molecular Graphics, *Acta Crystallogr. D50*, 869−873.
19. Ost, T. W. B., Miles, C. S., Munro, A. W., Murdoch, J., Reid, G. A., and Chapman, S. K. (2001) Phenylalanine 393 exerts thermodynamic control over the heme of flavocytochrome P450BM3, *Biochemistry 40*, 13421−13429.
20. Poulos, T. L., Finzel, B. C., Gunsalus, I. C., Wagner, G. C., and Kraut, J. (1985) The 2.6-Å crystal structure of *Pseudomonas putida* cytochrome P-450, *J. Biol. Chem. 260*, 16122−16130.
21. Imai, M., Shimada, H., Watanabe, Y., Matsushima-Hibiya, Y., Makino, R., Koga, H., Horiuchi, T., and Ishimura, Y. (1989) Uncoupling of the cytochrome P-450cam monooxygenase reaction by a single mutation, threonine-252 to alanine or valine: possible role of the hydroxy amino acid in oxygen activation, *Proc. Natl. Acad. Sci. U.S.A 86*, 7823−7827.
22. Gerber, N. S., and Sligar, S. G. (1992) Catalytic mechanism of cytrochrome P450 − evidence for a distal charge relay system, *J. Am. Chem. Soc. 114*, 8742−8743.
23. Kimata, Y., Shimada, H., Hirose, T., and Ishimura, Y. (1995) Role of Thr-252 in cytochrome P450cam: a study with unnatural amino acid mutagenesis, *Biochem. Biophys. Res. Commun. 208*, 96−102.
24. Raag, R., Martinis, S. A., Sligar, S. G., and Poulos, T. L. (1991) Crystal structure of the cytochrome P-450CAM active site mutant Thr252Ala, *Biochemistry 30*, 11420−11429.
25. Cupp-Vickery, J. R., Han, O., Hutchinson, C. R., and Poulos, T. L. (1996) Substrate-assisted catalysis in cytochrome P450eryF, *Nat. Struct. Biol. 3*, 632−627.
26. Vidakovic, M., Sligar, S. G., Li, H., and Poulos, T. L. (1998) Understanding the role of the essential Asp251 in cytochrome P450cam using site-directed mutagenesis, crystallography, and kinetic solvent isotope effect, *Biochemistry 37*, 9211−9219.
27. Gunsalus, I. C., Pederson, T. C., and Sligar, S. G. (1975) Oxygenase-catalyzed biological hydroxylations, *Annu. Rev. Biochem. 44*, 377−407.
28. Sevrioukova, I. F., Li, H., Zhang, H., Peterson, J. A., and Poulos, T. L. (1999) Structure of a cytochrome P450-redox partner electron-transfer complex, *Proc. Natl. Acad. Sci. U.S.A. 96*, 1863−1868.
29. Holden, M., Mayhew, M., Bunk, D., Roitberg, A., and Vilker, V. (1997) Probing the interactions of putidaredoxin with redox partners in camphor P450 5-monooxygenase by mutagenesis of surface residues, *J. Biol. Chem. 272*, 21720−21725.
30. Pochapsky, T. C., Ye, X. M., Ratnaswamy, G., and Lyons, T. A. (1994) An NMR-derived model for the solution structure of oxidized putidaredoxin, a 2-Fe, 2-S ferredoxin from *Pseudomonas*, *Biochemistry 33*, 6424−6232.
31. Pochapsky, T. C., Lyons, T. A., Kazanis, S., Arakaki, T., and Ratnaswamy, G. (1996) A structure-based model for cytochrome P450cam-putidaredoxin interactions, *Biochimie 78*, 723−733.
32. Atkins, W. M., and Sligar, S. G. (1988) The roles of active site hydrogen bonding in cytochrome P-450cam as revealed by site-directed mutagenesis, *J. Biol. Chem. 263*, 18842−18849.

BI049293P